

## Synthesis and DFT Quantum Chemical Calculations of 2-Oxopyrimidin-1(2H)-yl-Urea and Thiourea Derivatives

<sup>1</sup>Murat Saracoglu\*, <sup>2</sup>Zulbiye Kokbudak, <sup>2</sup>Esra Yalcin and <sup>3</sup>Fatma Kandemirli

<sup>1</sup>Erciyes University, Faculty of Education, 38039, Kayseri, Turkey.

<sup>2</sup>Erciyes University, Faculty of Science, 38039, Kayseri, Turkey.

<sup>3</sup>Kastamonu University, Faculty of Engineering and Architecture, 37150, Kastamonu, Turkey.

muratsaracoglu@gmail.com\*

(Received on 20<sup>th</sup> April 2018, accepted in revised form 26<sup>th</sup> February 2019)

**Summary:** A series of the new 2-oxopyrimidin-1(2H)-yl-urea (**3a-c**) and thiourea (**4a-d**) derivatives were synthesized by the reaction of arylisocyanates (**2a-c**) or arylisothiocyanates (**2d-g**) and the 1-amino-5-(4-methoxybenzoyl)-4-(4-methoxyphenyl)pyrimidin-2(1H)-one (**1**). The structures of the compounds **3a-c** and **4a-d** were characterized by elemental analysis, FT-IR, <sup>1</sup>H and <sup>13</sup>C-NMR spectroscopic techniques. In addition to experimental study in order to find molecular properties, quantum-chemical calculations of the synthesized compounds were carried out by using DFT/B3LYP method with basis set of the 6-311G(d,p). Quantum chemical features such as HOMO, LUMO, HOMO-LUMO energy gap, Ionization potential, chemical hardness, chemical softness, electronegativity, chemical potential, dipole moment etc. values for gas and solvent phase of neutral molecules were calculated and discussed.

**Keywords:** Urea and thiourea; Synthesis; DFT; Quantum chemical calculations.

### Introduction

Pyrimidines and its derivatives as important fine chemicals [1, 2] have been frequently found in many natural products and drugs and have exhibited a wide range of biological activities, such as anticancer [3], anti-inflammatory properties [4], antibacterial [5] and adenosine receptor antagonists [6]. Isothiocyanates and isocyanates are widely used for synthesis of heterocyclic compounds containing nitrogen, sulphur and oxygen. They also have industrial and pharmaceutical interest [7, 8].

Thioureas are important sulphur and nitrogen-containing compounds that have proved to be useful substances in drug research in recent years. They have been the subject of extensive study in coordination chemistry, and are also known to play a promising role in the fields of material sciences, molecular electronics, molecular recognition, agriculture, biological activities and pharmaceuticals. The presence of both soft and hard donors within the same molecular framework facilitates title compounds to be applied as ion sensors and transition metal extractors [9]. 1-(Acyl/aryl)-3-(substituted)thioureas have also emerged as attractive candidates in various fields such as ion sensors, in pharmaceuticals. The medicinal chemistry of this organo-sulfur framework has witnessed fantastic progress in the current era [10]. Some urea derivatives possess valuable anti-tuberculosis, antibacterial and anticonvulsant properties [11-14]. Many reported examples have demonstrated the varied biological activities of

thioureas, such as antitumor, antiviral, antimicrobial, antiparasitic, insecticidal, herbicidal, pesticidal and fungicidal properties. The 1H-benzimidazol thiourea derivatives evolved as promising anti-HIV and antibacterial agents. A wide array of pharmacological properties associated with 1-(acyl/aryl)-3-(substituted)thioureas has made them attractive templates for future drug design [9].

Considering the biological activities of these compounds, in this study a series of the new 2-oxopyrimidin-1(2H)-yl-urea (**3a-c**) and thiourea (**4a-d**) derivatives bearing pyrimidine rings were prepared from the reactions between 1-amino-5-(4-methoxybenzoyl)-4-(4-methoxyphenyl)pyrimidin-2(1H)-one (**1**) and the various arylisothiocyanates and arylisocyanates **2a-g** according to (Scheme-1). The synthesized compounds are shown in Table-1.

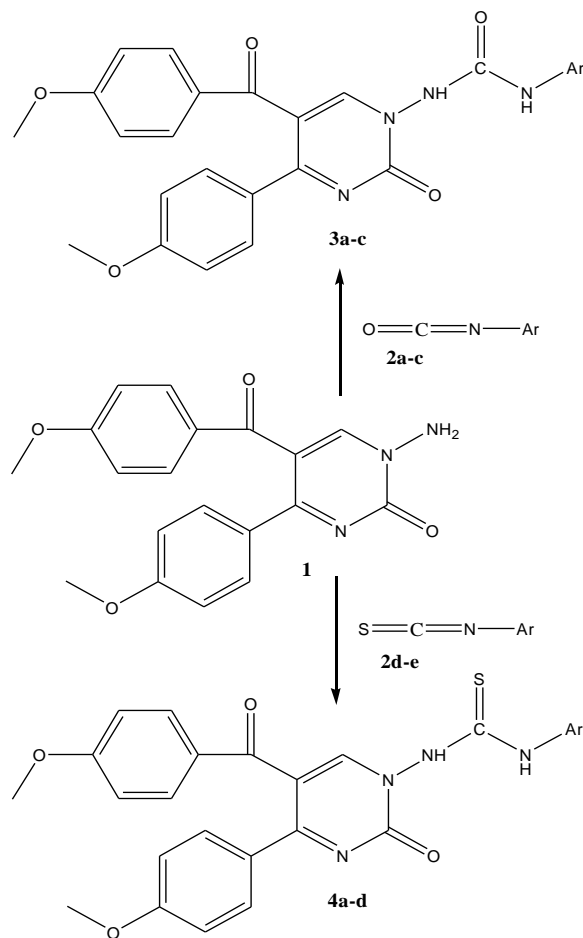
### Experimental

#### General materials and instruments

Chemicals and all solvents were commercially available and used without further purification. Melting points were determined on the digital melting point apparatus (Electrothermal 9100) and are uncorrected. The compounds were routinely checked for their homogeneity by TLC using DC Alufolien Kieselgel 60 F254 (Merck) and Camag TLC lamp (254/366 nm). Microanalyses were performed on a Leco CHNSO-932 Elemental

\*To whom all correspondence should be addressed.

Analysed and the results agreed favourably with the calculated values. The IR spectra were recorded on a Shimadzu Model 8400 FT-IR spectrophotometer. The  $^1\text{H}$  and  $^{13}\text{C}$ -NMR spectra were recorded on a Bruker 400(100) MHz Ultra Shield instrument. The chemical shifts are reported in ppm from tetramethylsilane as an internal standard and are given in  $\delta$  (ppm).

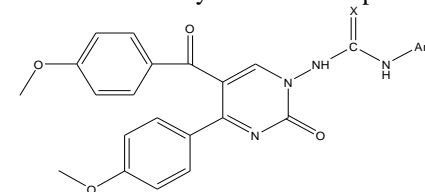


Scheme-1: The reaction for the formation of the products.

*General Procedure for the Preparation of 2-oxopyrimidin-1(2H)-yl-urea (3a-c) and thiourea (4a-d) derivatives*

Compound **1** and the corresponding of arylisothiocyanates or arylisocyanates **2a-g** (molar ratio 1:5 approximately) were homogeneously mixed in a 100 mL reaction flask. After the mixture was heated at 80-120 °C and kept at this temperature for 1-4 hour without any solvent. After cooling to room temperature, the residue was treated with dry ether and the resultant precipitate **3a-c** and **4a-d** were collected by filtration and recrystallized from a suitable solvent (ethanol and acetic acid).

Table-1: Structures of synthesized compounds.

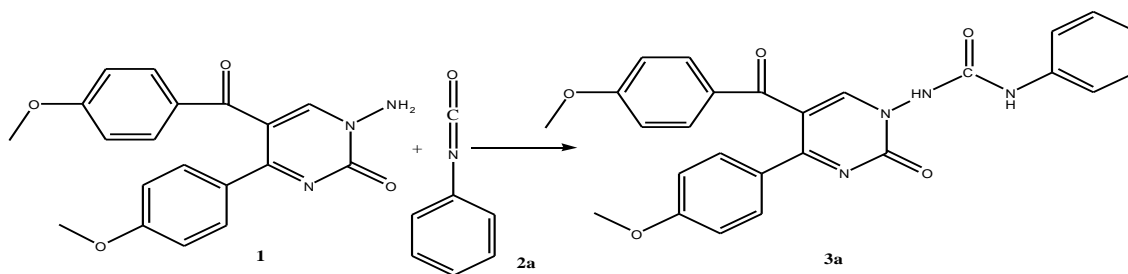


Compound	X	Ar
3a	O	Ph-
3b	O	4-CH <sub>3</sub> O-C <sub>6</sub> H <sub>4</sub> -
3c	O	4-Cl-C <sub>6</sub> H <sub>4</sub> -
4a	S	Ph-
4b	S	4-CH <sub>3</sub> O-C <sub>6</sub> H <sub>4</sub> -
4c	S	4-CH <sub>3</sub> -C <sub>6</sub> H <sub>4</sub> -
4d	S	1-naphthyl-

*Synthesis of 2-oxopyrimidin-1(2H)-yl-urea derivatives (3a-c)*

*1-(5-(4-Methoxybenzoyl)-4-(4-methoxyphenyl)-2-oxopyrimidin-1(2H)-yl)-3-phenylurea (3a)*

Product was recrystallized with ethanol and dried on P<sub>2</sub>O<sub>5</sub>; 68% yield (0.240 g); m.p. 230-232 °C (Scheme-2). FT-IR  $\nu$  (cm<sup>-1</sup>): 3229 (-NH), 3080 (arom. C-H stretch.), 2922 (aliph. C-H), 1716-1645 (3C=O), 1602-1591 (C=C and C=N), 740-660 (pyrim. ring skeleton vib.). Elemental analysis (%) for C<sub>26</sub>H<sub>22</sub>N<sub>4</sub>O<sub>5</sub>, Found (Calc.): C= 66.37 (66.18); H= 4.71 (4.64); N= 11.91 (11.75).



Scheme-2: The reaction for the formation of the **3a**.

$^1\text{H-NMR}$  (400 MHz, DMSO):  $\delta$ = 9.49, 9.47 (s, 2H, NH), 8.59 (s, 1H, pyrim. ring), 7.80-6.90 (m, 13H, Ar-H), 3.81-3.79 ppm (s, 6H, 2CH<sub>3</sub>O-).  $^{13}\text{C-NMR}$  (100 MHz, DMSO):  $\delta$ = 190.5 (4-CH<sub>3</sub>O-C<sub>6</sub>H<sub>4</sub>-C=O), 153.7 (NH-C=O), 153.6 (pyrim. C=O), 171.5-114.3 (pyrim. carbons and arom. carbons), 56.1-55.8 ppm (2CH<sub>3</sub>O-).

*1-(5-(4-Methoxybenzoyl)-4-(4-methoxyphenyl)-2-oxopyrimidin-1(2H)-yl)-3-(4-methoxyphenyl)urea (3b)*

Product was recrystallized with ethanol and dried on P<sub>2</sub>O<sub>5</sub>; 76% yield (0.270 g); m.p. 218-220 °C (Scheme-3). FT-IR  $\nu$  (cm<sup>-1</sup>): 3230 (NH), 3059 (arom. C-H stretch.), 2947 (aliph. C-H), 1717-1651 (3C=O), 1595-1550 (C=C and C=N), 680-820 (pyrim. ring skeleton vib.). Elemental analysis (%) for C<sub>27</sub>H<sub>24</sub>N<sub>4</sub>O<sub>6</sub>, Found (Calc.): C= 64.79 (64.60); H= 4.83 (4.74); N= 11.19 (11.10).

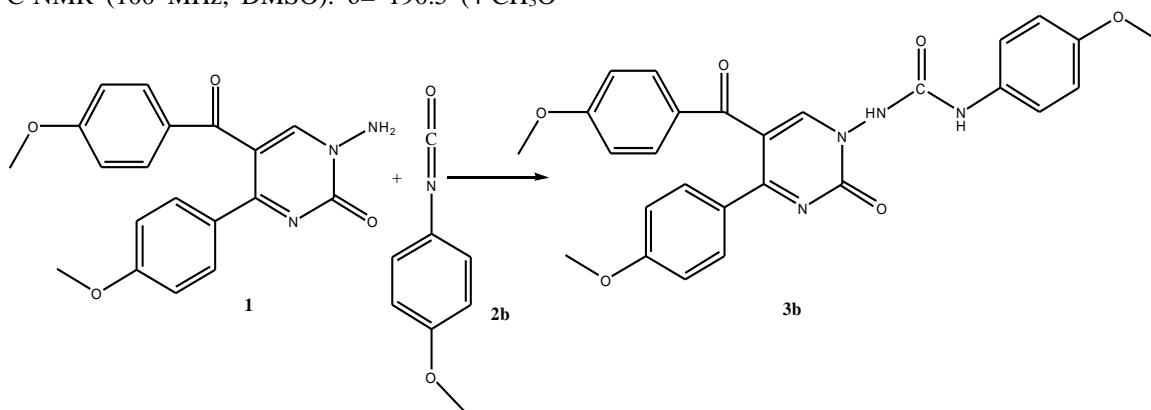
$^1\text{H-NMR}$  (400 MHz, DMSO):  $\delta$ = 9.42, 9.28 (s, 2H, NH), 8.47 (s, 1H, pyr. ring), 7.80-6.92 (m, 12H, Ar-H), 3.82, 3.75, 3.72 ppm (s, 9H, 3CH<sub>3</sub>O-).  $^{13}\text{C-NMR}$  (100 MHz, DMSO):  $\delta$ = 190.5 (4-CH<sub>3</sub>O-

C<sub>6</sub>H<sub>4</sub>-C=O), 153.8 (NH-C=O), 153.6 (pyrim. C=O), 171.5-114.3 (pyrim. carbons and arom. carbons), 56.1, 55.8, 55.6 ppm (3CH<sub>3</sub>O-).

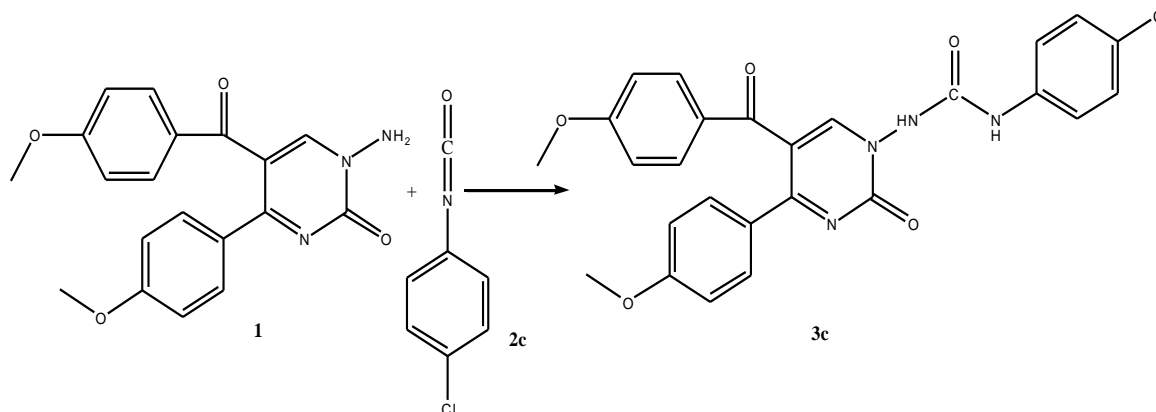
*1-(5-(4-Methoxybenzoyl)-4-(4-methoxyphenyl)-2-oxopyrimidin-1(2H)-yl)-3-(4-chlorophenyl)urea (3c)*

Product was recrystallized with acetic acid and dried on P<sub>2</sub>O<sub>5</sub>; 72% yield (0.255 g); m.p. 252-254 °C (Scheme-4). FT-IR  $\nu$  (cm<sup>-1</sup>): 3247 (NH), 3040 (arom. C-H), 2964 (aliph. C-H), 1728-1651 (3C=O), 1601-1596 (C=C and C=N), 820-700 (pyrim. ring skeleton vib.). Elemental analysis (%) for C<sub>26</sub>H<sub>21</sub>N<sub>4</sub>O<sub>5</sub>Cl, Found (Calc.): C= 61.85 (61.60); H= 4.19 (4.04); N= 11.10 (11.05), Cl= 7.02 (6.85).

$^1\text{H-NMR}$  (400 MHz, DMSO):  $\delta$ = 9.59, 9.58 (s, 2H, NH), 8.47 (s, 1H, pyrim. ring), 7.79-6.90 (m, 12H, Ar-H), 3.81, 3.74 ppm (s, 6H, 2CH<sub>3</sub>O-).  $^{13}\text{C-NMR}$  (100 MHz, DMSO):  $\delta$ = 190.4 (4-CH<sub>3</sub>O-C<sub>6</sub>H<sub>4</sub>-C=O), 153.7 (NH-C=O), 153.5 (pyrim. C=O), 171.6-114.3 (pyrim. carbons and arom. carbons), 55.8, 56.1 ppm (2CH<sub>3</sub>O-).



Scheme-3: The reaction for the formation of the **3b**.



Scheme-4: The reaction for the formation of the **3c**.

*Synthesis of 2-oxopyrimidin-1(2H)-yl-thiourea derivatives (4a-d)*

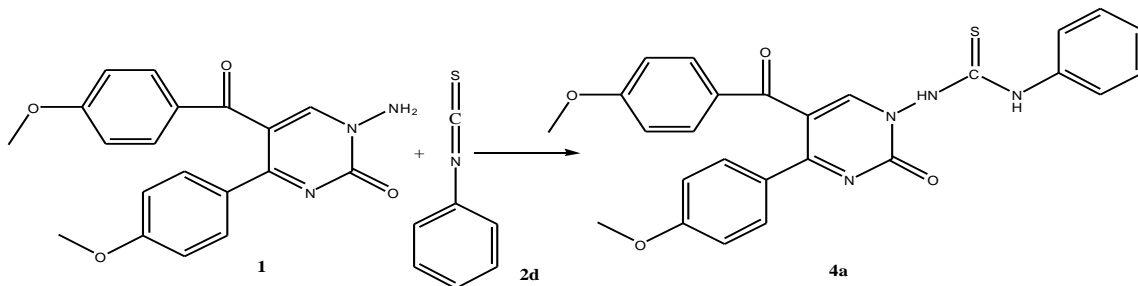
*1-(5-(4-Methoxybenzoyl)-4-(4-methoxyphenyl)-2-oxopyrimidin-1(2H)-yl)-3-phenylthiourea (4a)*

Product was recrystallized with ethanol and dried on P<sub>2</sub>O<sub>5</sub>; 72% yield (0.255 g); m.p. 210-212 °C (Scheme-5). FT-IR  $\nu$  (cm<sup>-1</sup>): 3267 (-NH), 3096 (arom. C-H stretch.), 2931 (aliph. C-H), 1734-1680 (2C=O), 1600-1591 (C=C and C=N), 740-660 (pyrim. ring skeleton vib.), 1258 (thiocarbonyl C=S). Elemental analysis (%) for C<sub>26</sub>H<sub>22</sub>N<sub>4</sub>O<sub>4</sub>S, Found (Calc.): C= 64.18 (64.08); H= 4.56 (4.34); N= 11.52 (11.40); S= 6.59 (6.40).

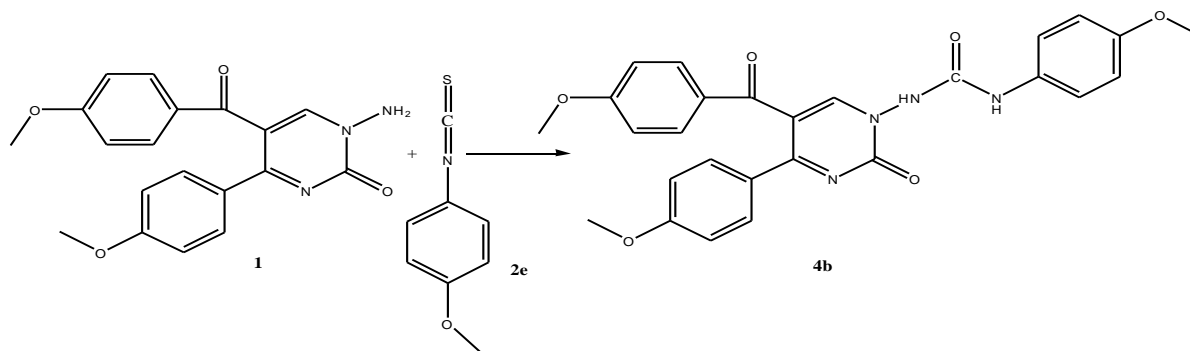
<sup>1</sup>H-NMR (400 MHz, DMSO):  $\delta$ = 10.81, 10.50 (s, 2H, NH), 8.47 (s, 1H, pyrim. ring), 7.87-6.67 (m, 13H, Ar-H), 3.83-3.75 ppm (s, 6H, 2CH<sub>3</sub>O-). <sup>13</sup>C-NMR (100 MHz, DMSO):  $\delta$ = 190.4 (4-CH<sub>3</sub>O-C<sub>6</sub>H<sub>4</sub>-C=O), 180.1 (NH-C=S), 152.9 (pyrim. C=O), 171.7-113.7 (pyrim. carbons and arom. carbons), 56.1-55.8 ppm (2CH<sub>3</sub>O-).

*1-(5-(4-Methoxybenzoyl)-4-(4-methoxyphenyl)-2-oxopyrimidin-1(2H)-yl)-3-(4-methoxyphenyl)thiourea (4b)*

Product was recrystallized with ethanol and dried on P<sub>2</sub>O<sub>5</sub>; 79% yield (0.280 g); m.p. 178-180 °C



Scheme-5: The reaction for the formation of the 4a.



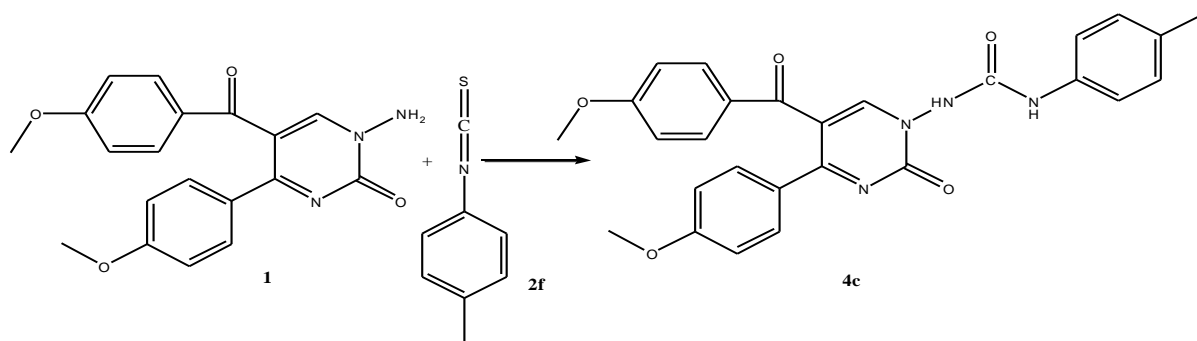
Scheme-6: The reaction for the formation of the 4b.

(Scheme-6). FT-IR  $\nu$  (cm<sup>-1</sup>): 3256 (NH), 3060 (arom. C-H stretch.), 2970 (aliph. C-H), 1738-1676 (2C=O), 1600-1581 (C=C and C=N), 1218 (thiocarbonyl C=S), 810-685 (pyrim. ring skeleton vib.). Elemental analysis (%) for C<sub>27</sub>H<sub>24</sub>N<sub>4</sub>O<sub>5</sub>S, Found (Calc.): C= 62.78 (62.60); H= 4.68 (4.57); N= 10.85 (10.60), S= 6.21 (6.10).

<sup>1</sup>H-NMR (400 MHz, DMSO):  $\delta$ = 10.80, 10.70 (s, 2H, NH), 8.44 (s, 1H, pyrim. ring), 7.86-6.68 (m, 12H, Ar-H), 3.83, 3.76, 3.74 ppm (s, 9H, 3CH<sub>3</sub>O-). <sup>13</sup>C-NMR (100 MHz, DMSO):  $\delta$ = 191.0 (4-CH<sub>3</sub>O-C<sub>6</sub>H<sub>4</sub>-C=O), 180.1 (NH-C=S), 152.9 (pyrim. C=O), 171.7-113.7 (pyrim. carbons and arom. carbons), 56.1, 55.8, 55.7 ppm (3CH<sub>3</sub>O-).

*1-(5-(4-Methoxybenzoyl)-4-(4-methoxyphenyl)-2-oxopyrimidin-1(2H)-yl)-3-(4-methoxyphenyl)thiourea (4c)*

Product was recrystallized with ethanol and dried on P<sub>2</sub>O<sub>5</sub>; 65% yield (0.230 g); m.p. 220-222 °C (Scheme-7). FT-IR  $\nu$  (cm<sup>-1</sup>): 3260 (NH), 3040 (arom. C-H), 2964 (aliph. C-H), 1742-1686 (2C=O), 1600-1580 (C=C and C=N), 1231 (thiocarbonyl C=S), 830-710 (pyrim. ring skeleton vib.). Elemental analysis (%) for C<sub>27</sub>H<sub>24</sub>N<sub>4</sub>O<sub>5</sub>S, Found (Calc.): C= 64.78 (64.56); H= 4.83 (4.65); N= 11.19 (11.02), S= 6.41 (6.33).

Scheme-7: The reaction for the formation of the **4c**.

$^1\text{H-NMR}$  (400 MHz, DMSO):  $\delta$ = 10.76, 10.45 (s, 2H, NH), 8.48 (s, 1H, pyrim. ring), 7.86-6.68 (m, 12H, Ar-H), 3.83, 3.75 (s, 6H, 2CH<sub>3</sub>O-), 2.53 ppm (s, 3H, -CH<sub>3</sub>).  $^{13}\text{C-NMR}$  (100 MHz, DMSO):  $\delta$ = 190.3 (4-CH<sub>3</sub>O-C<sub>6</sub>H<sub>4</sub>-C=O), 180.1 (NH-C=S), 153.1 (pyrim. C=O), 171.4-114.1 (pyrim. carbons and arom. carbons), 56.1, 55.8 ppm (2CH<sub>3</sub>O-).

171.8-114.3 (pyrim. carbons and arom. carbons), 56.1-55.8 ppm (2CH<sub>3</sub>O-).

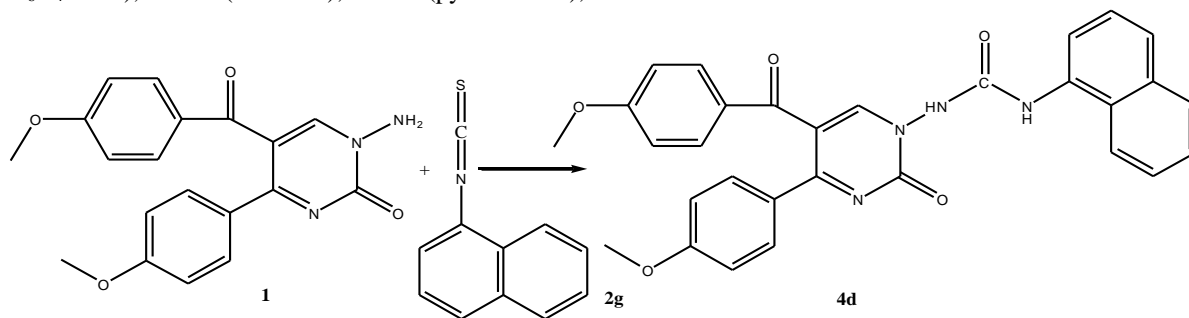
#### Computational details

In this section of study, all calculations were carried out by using DFT/B3LYP method. Optimization of synthesized molecules was performed with 6-311G(d,p) basis set of Gaussian 03, Revision D.01 program [15]. This basis set is known as one of the basis sets that gives more accurate results in terms of the determination of electronic and geometries properties for a wide range of organic compounds [16]. Quantum chemical parameters for synthesized molecules such as; the energy of the highest occupied molecular orbital ( $E_{\text{HOMO}}$ ), the energy of the lowest unoccupied molecular orbital ( $E_{\text{LUMO}}$ ), HOMO-LUMO energy gap ( $\Delta E$ ), ionization potential (I), chemical hardness ( $\eta$ ), softness ( $\sigma$ ), electronegativity ( $\chi$ ), chemical potential ( $\mu$ ), dipole moment (DM), global electrophilicity ( $\omega$ ) and total of negative Mulliken atomic charges (TMAC), Mulliken charges of some atoms for gas and solvent phase of neutral molecules were calculated and discussed. Recently, the optimization of the molecules with different basic groups and the discussion of the results have been widely used [17-37].

#### 1-(5-(4-Methoxybenzoyl)-4-(4-methoxyphenyl)-2-oxopyrimidin-1(2H)-yl)-3-(naphthalen-1-yl)thiourea (**4d**)

Product was recrystallized with ethanol and dried on P<sub>2</sub>O<sub>5</sub>; 62% yield (0.220 g); m.p. 190-192 °C (Scheme-8). FT-IR  $\nu$  (cm<sup>-1</sup>): 3240 (NH), 3061 (arom. C-H), 2978 (aliph. C-H), 1742-1686 (2C=O), 1603-1591 (C=C and C=N), 1249 (thiocarbonyl C=S) 830-710 (pyrim. ring skeleton vib.). Elemental analysis (%) for C<sub>30</sub>H<sub>24</sub>N<sub>4</sub>O<sub>4</sub>S, Found (Calc.): C= 67.15 (67.01); H= 4.51 (4.31); N= 10.44 (10.24), S= 5.98 (5.76).

$^1\text{H-NMR}$  (400 MHz, DMSO):  $\delta$ = 10.94, 10.57 (s, 2H, NH), 8.62 (s, 1H, pyrim. ring), 7.97-6.94 (m, 15H, Ar-H), 3.84, 3.72 ppm (s, 6H, 2CH<sub>3</sub>O-).  $^{13}\text{C-NMR}$  (100 MHz, DMSO):  $\delta$ = 190.5 (4-CH<sub>3</sub>O-C<sub>6</sub>H<sub>4</sub>-C=O), 180.1 (NH-C=S), 153.0 (pyrim. C=O),

Scheme-8: The reaction for the formation of the **4d**.

Molecular properties, related to the reactivity and selectivity of the compounds, were estimated following the Koopmans's theorem [38] relating the energy of the HOMO and the LUMO. According to the DFT-Koopmans' theorem [38, 39], the ionization potential (I) can be approximated as the negative value of the highest occupied molecular orbital energy ( $E_{\text{HOMO}}$ ), such as shown in equation 1:

$$I = -E_{\text{HOMO}} \quad (1)$$

The negative value of the lowest unoccupied molecular orbital energy ( $E_{\text{LUMO}}$ ) is similarly related to the electron affinity A [40] such as shown in equation 2:

$$A = -E_{\text{LUMO}} \quad (2)$$

Energy gap ( $\Delta E$ ) is estimated by using the  $E_{\text{HOMO}}$  and  $E_{\text{LUMO}}$ :

$$\Delta E = E_{\text{LUMO}} - E_{\text{HOMO}} \quad (3)$$

Electronegativity ( $\chi$ ) is estimated using the following the equation from  $E_{\text{HOMO}}$  and  $E_{\text{LUMO}}$  [41] or I and A [42]:

$$\chi \cong -\left(\frac{E_{\text{HOMO}} + E_{\text{LUMO}}}{2}\right) = \left(\frac{I + A}{2}\right) \quad (4)$$

Chemical hardness ( $\eta$ ) measures the resistance of an atom to a charge transfer [41], it's estimated by using the equation from  $E_{\text{HOMO}}$  and  $E_{\text{LUMO}}$  or I and A [42]:

$$\eta \cong -\left(\frac{E_{\text{HOMO}} - E_{\text{LUMO}}}{2}\right) = \left(\frac{I - A}{2}\right) \quad (5)$$

Electron polarizability, called chemical softness ( $\sigma$ ), describes the capacity of an atom or group of atoms to receive electrons [41] and is estimated by using the equation:

$$\sigma = \frac{1}{\eta} \cong -\left(\frac{2}{E_{\text{HOMO}} - E_{\text{LUMO}}}\right) \quad (6)$$

Chemical potential ( $\mu$ ) and electronegativity ( $\chi$ ) can be calculated with the help of the following equations [16] from  $E_{\text{HOMO}}$  and  $E_{\text{LUMO}}$ :

$$\mu = -\chi \cong \left(\frac{E_{\text{HOMO}} + E_{\text{LUMO}}}{2}\right) \quad (7)$$

The global electrophilicity index ( $\omega$ ) is a useful reactivity descriptor that can be used to compare the electron-donating abilities of molecules [43]. Global electrophilicity index is estimated by using the electronegativity and chemical hardness parameters through the equation:

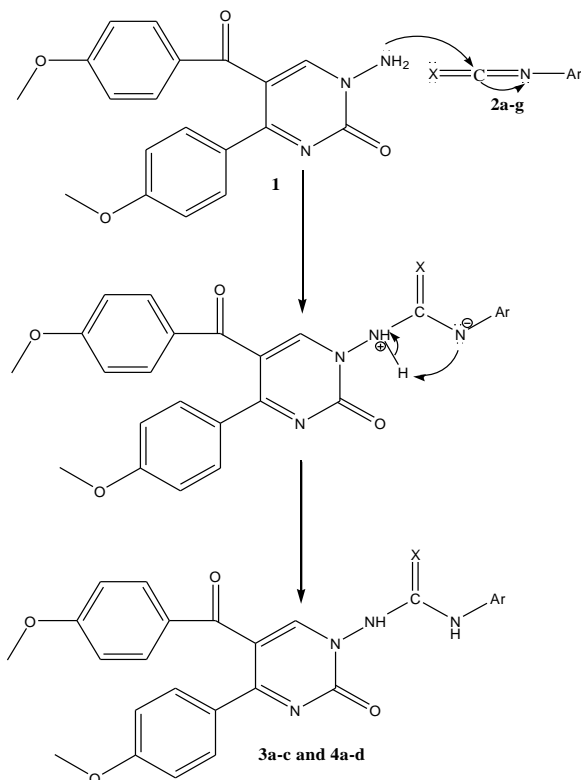
$$\omega = \frac{\chi^2}{2\eta} \quad (8)$$

A high value of electrophilicity describes a good electrophile while a small value of electrophilicity describes a good nucleophile [44].

## Results and discussion

### Structural analysis

The new 2-oxypyrimidin-1(2*H*)-yl-urea (**3a-c**) and thiourea (**4a-d**) derivatives (Scheme-1) were isolated in satisfactory yields (62–79%) from nucleophilic addition of **1** to the corresponding arylisocyanates and arylisothiocyanates (**2a-g**) [8]. The compound **1** was synthesized in two steps from 4-(4-methoxybenzoyl)-5-(4-methoxyphenyl)furan-2,3-dione [45]. All compounds readily were purified by recrystallization. The moderate yield of the reactions can be explained by the chemical behaviour of 4,5-substituted pyrimidine-2-one (**1**) towards the compounds **2a-g**. The carbon atoms represent the electrophilic site in the molecules of the isothiocyanates and the isocyanates so they can be interacted with nucleophiles (Scheme-2). The nucleophilic attack of the amino group of the 4,5-substituted pyrimidine-2-one **1** on carbonyl and thiocarbonyl groups of isocyanate and isothiocyanate leads to formation of an intermediate. During the consecutive steps, deprotonation and protonation of the intermediate results in the formation of the final products urea (**3a-c**) and thiourea (**4a-d**) derivatives (Scheme-9). The reactions were performed heating without solvent up to (80-120 °C) (see experimental section). The structures of the new synthesized **3a-c** and **4a-d** compounds were characterized using elemental analysis, <sup>1</sup>H-NMR, <sup>13</sup>C-NMR and FT-IR spectroscopic techniques.



Scheme-9: The mechanism for the formation of the products.

*Structural analysis of 2-oxopyrimidin-1(2H)-yl-urea derivatives (3a-c)*

*1-(5-(4-Methoxybenzoyl)-4-(4-methoxyphenyl)-2-oxopyrimidin-1(2H)-yl)-3-phenylurea (3a)*

The compound **3a** was obtained from the reaction of compound **1** and phenylisocyanate **2a** in 68% yield. The IR spectrum of compound **3a** showed the presence of NH groups at 3229  $\text{cm}^{-1}$ . The IR spectrum of compound **3a** showed significant characteristic stretching bands to the C=O groups (benzoyl, pyrimidine structure and urea). These band observed at 1716-1645  $\text{cm}^{-1}$ . In the  $^1\text{H-NMR}$  spectrum, NH protons of urea groups in the structure of compound **3a**, resonated at 9.49 ppm (s, 2H, NH). Moreover, disappearance of broad singlet at 5.14 ppm  $\text{NH}_2$  proton of compound **3a** clearly confirmed the formation of urea derivatives [45]. The aromatic protons of **3a** were observed in the 7.80-6.90 ppm region as multiplet. The signals of methoxy protons in the structure of **3a** were observed at 3.81, 3.79 ppm as singlets. Resonated signals were recorded by  $^{13}\text{C-NMR}$  spectrum at 190.5 (4- $\text{CH}_3\text{O-C}_6\text{H}_4\text{-C=O}$ ), 153.6 (pyrim. C=O) and 153.7 ppm (NH-C=O) due to the presence of C=O carbons [46-48]. The signals of

$\text{CH}_3\text{O}$ -groups were observed at 56.1, 55.8 ppm and aromatic carbons were determined in the 171.5-114.3 ppm region.

*1-(5-(4-Methoxybenzoyl)-4-(4-methoxyphenyl)-2-oxopyrimidin-1(2H)-yl)-3-(4-methoxyphenyl)urea (3b)*

The compound **3b** was synthesized from the reaction of compound **1** and 4-methoxyphenylisocyanate **2b** in 76% yield. According to the IR spectrum of **3b**, the absorption bands at 3230, 1717, 1651  $\text{cm}^{-1}$  indicated to presence of NH and three C=O groups, respectively. The NH peaks were seen at 9.42, 9.28 ppm as singlets. The  $^1\text{H-NMR}$  spectrum of **3b** demonstrated singlets for the protons of methoxy groups at 3.82, 3.75, 3.72 ppm and multiplet for aromatic protons at 7.80-6.92 ppm region. The signals of carbonyl carbons were observed at 190.5 (4- $\text{CH}_3\text{O-C}_6\text{H}_4\text{-C=O}$ ), 153.6 (pyrim. C=O) and 153.8 (NH-C=O) ppm. The signals aromatic carbons were observed at of 171.5-114.3 ppm and the signals of methoxy carbons were observed at 56.1, 55.8 and 55.6 ppm as singlets [46, 47].

*1-(5-(4-Methoxybenzoyl)-4-(4-methoxyphenyl)-2-oxopyrimidin-1(2H)-yl)-3-(4-chlorophenyl)urea (3c)*

The compound **3c** was synthesized from the reaction of compound **1** and 4-chlorophenylisocyanate **2c** in 72% yield. The IR spectrum of **3c** exhibited stretching band at 3247 and 1728-1651  $\text{cm}^{-1}$  for the NH and the C=O groups. The NH peaks of **3c** were seen at 9.59, 9.58 ppm as singlets. Multiplet for aromatic protons at 7.79-6.90 ppm region and singlets at 3.81, 3.74 ppm for the methoxy groups were observed. Resonated signals were recorded by  $^{13}\text{C-NMR}$  spectrum at 190.4 (4- $\text{CH}_3\text{O-C}_6\text{H}_4\text{-C=O}$ ), 153.5 (pyrim. C=O) and 153.7 ppm (NH-C=O) due to the presence of C=O carbons. The signals of  $\text{CH}_3\text{O}$ - groups were observed at 55.8, 56.1 ppm as singlets and aromatic carbons at 171.6-114.3 ppm region as multiplet [47].

*Structural analysis of 2-oxopyrimidin-1(2H)-yl-thiourea derivatives (4a-d)*

*1-(5-(4-Methoxybenzoyl)-4-(4-methoxyphenyl)-2-oxopyrimidin-1(2H)-yl)-3-phenylthiourea (4a)*

The compound **4a** was obtained from the reaction of compound **1** and phenylisothiocyanate **2d** in 72% yield. The IR spectrum of **4a** exhibited stretching band at 3267, 1734 and 1680  $\text{cm}^{-1}$  for

the two NH and the two C=O groups. The formation of **4a** were confirmed by the absence of characteristic infrared absorption peak at 2000-2200  $\text{cm}^{-1}$  (N=C=S group). According to the IR spectrum of **4a**, the absorption band at 1258  $\text{cm}^{-1}$  indicated the presence C=S group. Thiocarbonyl is less polar than the carbonyl group and the link C=S is weaker and it is located at lower frequencies than carbonyl [46, 48]. The  $^1\text{H}$ -NMR spectrum of **4a** revealed signals at 10.81, 10.50 ppm for two protons of NH (thiourea), 8.47 ppm (singlet the proton of pyrim.), 7.87-6.67 ppm (multiplet for aromatic protons), and 3.83 and 3.75 ppm (singlets for methoxy groups protons).  $^{13}\text{C}$ -NMR spectrum of **4a** showed signals at 190.4, 180.1, 152.9 ppm which were assigned to 4- $\text{CH}_3\text{O}$ - $\text{C}_6\text{H}_4$ -C=O, NH-C=S, C=O (pyrim.), respectively. The signals for methoxy carbons were observed at 56.1 and 55.8 ppm. Aromatic carbons were observed in the region of 171.8-113.7 ppm.

*1-(5-(4-Methoxybenzoyl)-4-(4-methoxyphenyl)-2-oxopyrimidin-1(2H)-yl)-3-(4-methoxyphenyl)thiourea (4b)*

The compound **4b** was synthesized from the reaction of compound **1** and 4-methoxyphenylisothiocyanate **2e** in 79% yield. The structure of **4b** was deduced from elemental analysis and spectral data. The IR absorptions showed the presence of NH (3256  $\text{cm}^{-1}$ ) and carbonyl groups (1738-1676  $\text{cm}^{-1}$ ). In addition, peak at 1218  $\text{cm}^{-1}$  were assigned to C=S group. The  $^1\text{H}$ -NMR spectrum of **4b** indicated the presence of two singlets at 10.80 and 10.70 ppm for NH protons of thiourea derivatives. The singlets for the protons of methoxy groups at 3.83, 3.76, 3.74 ppm and multiplet for aromatic protons at 7.86-6.68 ppm region were observed.  $^{13}\text{C}$ -NMR spectra showed highest frequency signal observed at 191.02 ppm to the benzoyl carbon.  $^{13}\text{C}$ -NMR spectrum showed signals at 180.1 ppm (NH-C=S) and 152.9 ppm (C=O, pyrim.), in addition, at 56.1, 55.8, 55.7 ppm of  $\text{CH}_3\text{O}$  groups with 171.7-113.7 ppm of aromatic carbons [46, 48].

*1-(5-(4-Methoxybenzoyl)-4-(4-methoxyphenyl)-2-oxopyrimidin-1(2H)-yl)-3-(4-methylphenyl)thiourea (4c)*

The compound **4c** was synthesized from the reaction of compound **1** and 4-methylphenylisothiocyanate **2f** in 65% yield. The IR spectrum of **4c** indicated the presence of NH (3260  $\text{cm}^{-1}$ ), carbonyls (1742 and 1686  $\text{cm}^{-1}$ ) and thiocarbonyl (1231  $\text{cm}^{-1}$ ) functional groups.  $^1\text{H}$ -

NMR spectrum of **4c** showed singlets at 10.76, 10.45 ppm for NH protons. The aromatic protons were observed in the region 7.86-6.68 ppm. The singlets were observed at 56.12-55.75 ppm for methoxy protons. The signals for carbonyl and C=S groups were observed at 190.3, 153.1 and 180.1 ppm, respectively [46, 48]. The signals of  $\text{CH}_3\text{O}$  groups were observed at 56.1, 55.8 ppm as singlets. Aromatic carbons were observed in the 171.4-113.2 ppm region.

*1-(5-(4-Methoxybenzoyl)-4-(4-methoxyphenyl)-2-oxopyrimidin-1(2H)-yl)-3-(naphthalen-1-yl)thiourea (4d)*

The compound **4d** was synthesized from the reaction of compound **1** and 1-naphthylisothiocyanate **2g** in 62% yield. The absorption bands at 3240, 1742, 1686 and 1249  $\text{cm}^{-1}$  in the IR spectrum of compound **4d** indicated the presence of NH, C=O groups and thiocarbonyl group. The  $^1\text{H}$ -NMR spectrum showed singlets at 10.94, 10.57 ppm for NH protons and multiplet at 7.97-6.94 ppm for aromatic protons and singlets at 3.84, 3.72 ppm for methoxy protons. The signals for carbonyl/thiocarbonyl carbons were observed at 190.5 (4- $\text{CH}_3\text{O}$ - $\text{C}_6\text{H}_4$ -C=O), 180.1 (NH-C=S) and 153.0 ppm (C=O, pyrim.) [46, 48]. The signals of  $\text{CH}_3\text{O}$ - groups were observed at 56.1, 55.8 ppm and aromatic carbons were observed in the 171.8-114.3 ppm region.

*Molecular structure*

$E_{\text{HOMO}}$ ,  $E_{\text{LUMO}}$ ,  $\Delta E$ , I,  $\eta$ ,  $\sigma$ , etc. values were calculated for the 2-oxopyrimidin-1(2H)-yl-urea derivatives (after that, it will be called as briefly urea derivatives or **3a-e**) and 2-oxopyrimidin-1(2H)-yl-thiourea derivatives (after that, it will be called as briefly thiourea derivatives or **4a-d**) with the DFT/B3LYP/6-311G(d,p) method for gas phase and solvent phase (acetic acid for **3c** and ethanol for other molecules) of neutral molecules, as shown in Figs. 1-4, and Table-2.

According to the frontier molecular orbital (FMO) theory, the chemical reactivity of molecule is a function of interaction between HOMO and LUMO levels of the reacting species [49]. HOMO and LUMO are known as frontier orbitals, and these a molecule play important role in the determination of its molecular reactivity or stability. Some researchers mention that Frontier orbital theory is useful in predicting the molecule's interaction center [50-52]. The FMOs (HOMOs,

LUMOs) of molecules are given in Fig. 1. It could be easily found that the HOMO distributions of molecules are mainly located all-around of **3a** and **3c** molecules. HOMO distributions of thiourea derivatives **4a-d**, it is located around of NH-C=S. The electron-rich regions of the molecule can be said to be more active. The presence of sulfur atoms on these molecules to be causes strong activity. Also, this fig shows that there is much more electron density in sulfur atoms of **4a-d** molecules. The results show that interaction of molecules with C=S bond in **4a-d** are easier. Obi-Egbedi and *et al.* showed that the C=S bond with the metal surface adsorbed more easily [53]. This indicates that these compounds can also be used as a corrosion inhibitor. It is important to note that the most effective corrosion inhibitors are  $\pi$ -systems and heterocyclic organic compounds including heteroatoms such as O, N, S [54]. Corrosion inhibition process can be described as the formation of donor-acceptor surface complexes between vacant *d*-orbital of a metal with free or  $\pi$ -electrons of organic inhibitor, generally including aforementioned heteroatoms [55]. The LUMO distributions of **3a-c** and **4a-d** molecules are mainly located around of the pyrimidine and non-carbonyl phenyl ring. The charge density distribution of HOMO and LUMO level of urea and thiourea derivatives for notr and solvent phase are shown in Fig. 1. Fig. 1 shows that the HOMO and LUMO orbitals are present in similar regions of notr and the solvent phase when we consider each compound separately.

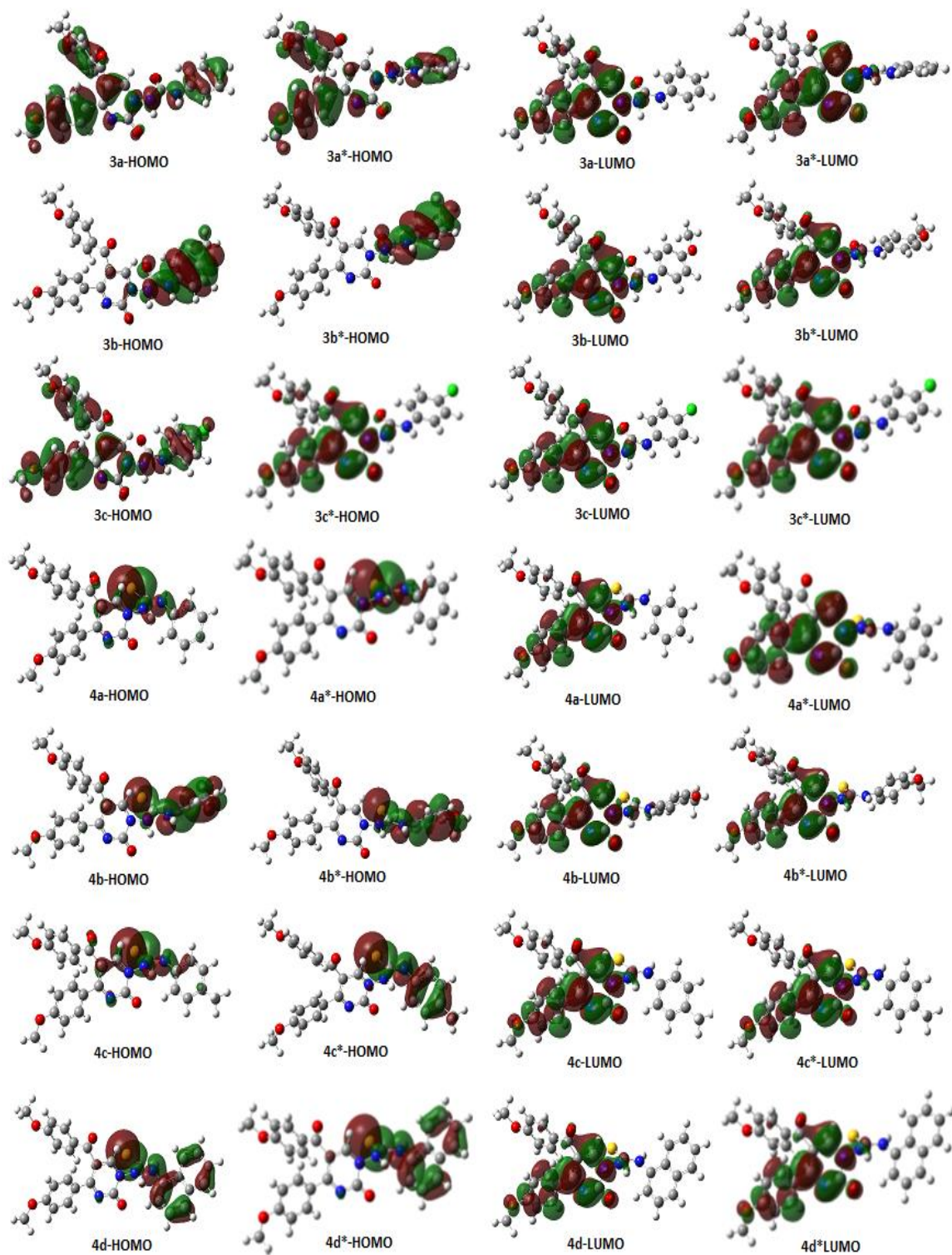
According to the frontier molecular orbital theory (FMO), the chemical reactivity of molecule is a function of interaction between HOMO and LUMO levels of the reacting species.  $E_{\text{HOMO}}$  and  $E_{\text{LUMO}}$  are associated with electron donating ability and electron accepting ability of a molecule, respectively. High  $E_{\text{HOMO}}$  is essential for reaction with nucleophiles of molecule while low  $E_{\text{LUMO}}$  is essential for reaction with electrophiles [56].

$E_{\text{HOMO}}$  values were found in gas phase for **3a-c** molecules of urea derivatives -6.18, -5.78, -6.24 eV, and -6.13, -5.95, -6.08, -6.11 eV for thiourea derivatives, respectively.  $E_{\text{HOMO}}$  values were found in solvent phase -6.25, -5.67, -6.21 for **3a-c** and -6.22, -6.04, -6.20, -6.11 eV for **4a-d**, respectively (Fig. 2). According to these results, the sequence of reactivity for gas phase of study molecules can be written as: **3c>3a>3b** for urea derivatives and **4a>4d>4c>4b** for thiourea derivatives, and solvent phase **3a>3c>3b** for **3a-c** and **4a>4c>4d>4b** for **4a-d** molecules.  $E_{\text{HOMO}}$  and

$E_{\text{LUMO}}$  values in **3b** and **4b** molecules are lower than other molecules. This condition is due to the methoxy group attached to the phenyl ring of **3b** and **4b** molecules. As is known, the methoxy group is an electron attracting group. There is no significant change in the  $E_{\text{HOMO}}$  and  $E_{\text{LUMO}}$  values for gas and solvent phase according to the position and number of groups in the ring expect for **3b** and **4b**.

HOMO-LUMO energy gap ( $\Delta E$ , see eq. 3), chemical hardness and softness are closely related to chemical properties [53, 57-60]. Chemical hardness introduced in 1960s by Pearson [54] is defined as the resistance towards electron cloud polarization or deformation of chemical species. According to the Maximum Hardness Principle states; "a chemical system tends to arrange itself so as to achieve maximum hardness and chemical hardness can be considered as a measurement of stability" [61]. The physical properties of the compounds are strongly dependent on the energy gap between the compounds. The large  $\Delta E$  indicates a high kinetic stability and also low molecular activity of the compound. Because, the higher  $\Delta E$  of the molecules are difficult to polarize. The compounds need more energy to excite but lower gaps of energy are relatively easy to polarize and it reacts more efficiently than higher values of energy gaps [62]. Pearson showed that hard molecules with a high  $\Delta E$  values are more stable compared to soft molecules with a low  $\Delta E$  values [63, 64]. The smaller  $\Delta E$  is often interpreted by a stronger activity and perhaps greater inhibition efficiency [50]. So,  $\Delta E$  decreases, the reactivity of the molecule increases leading to a better inhibition efficiency and activity [60].

$\Delta E$  values for gas phase were found 4.20, 3.84, 4.18 of **3a-c** molecules and 4.10, 4.00, 4.08, 4.09 eV of **4a-d** molecules, respectively, and for solvent phase 4.06, 3.57, 4.11 of **3a-c** and 4.05, 3.91, 3.95, 4.18 eV of **4a-d**, respectively.  $\Delta E$  values in the solvent phase are lower than the notr phase for **3a-c** and **4a-d** molecules. Therefore, the solvent phase is expected to be more active. **3b** and **4b** molecules are found more active than other molecules for gas and solvent phase due to the fact that a low  $\Delta E$  value is observed (Fig. 2). It appears that the most active compound is **3b** for urea derivatives in notr and solvent phase and **4b** for thiourea derivatives in notr and solvent phase. Because, it can be seen from values that **3b** and **4b** molecules have the lowest  $\Delta E$  values.



\*Solvent phase: acetic acid for **3c** and ethanol for other molecules.

Fig. 1: The frontier MOs (HOMOs, LUMOs) molecules by using DFT/B3LYP/6-311G(d,p) basic set for notr and solvent phase.

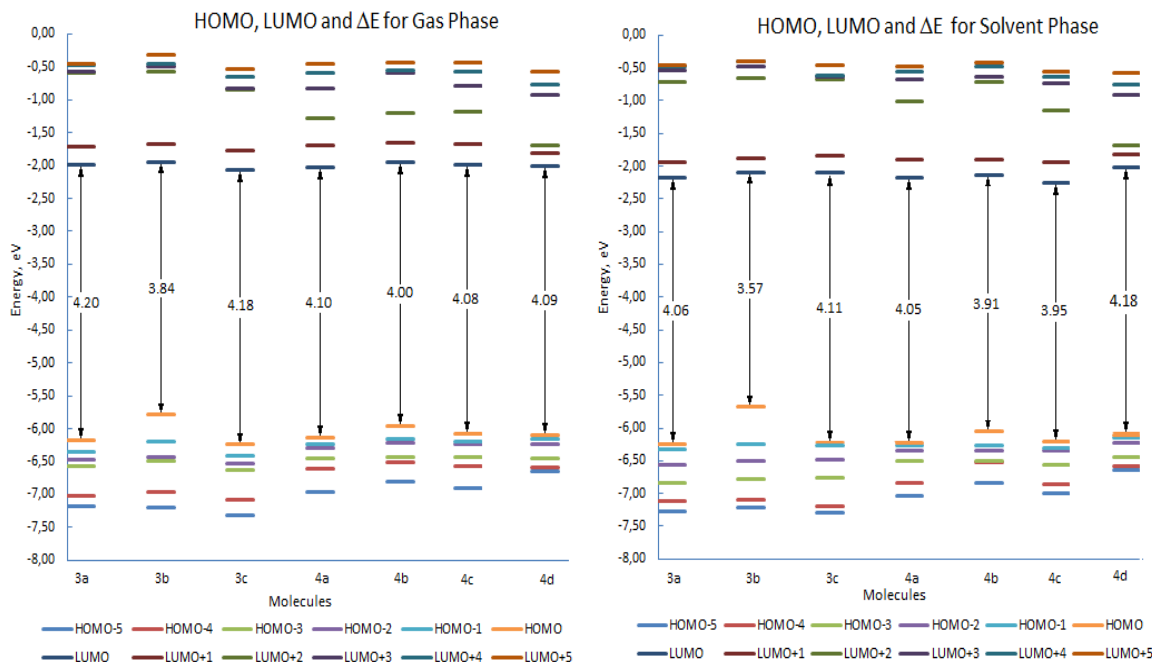


Fig. 2: The calculated HOMO, LUMO and energy gap parameters for gas and solvent phase of neutral molecules using B3LYP/6-311G(d,p) method.

Ionization potential (I) is one of the fundamental indicators of the chemical reactivity. High values of the ionization potential (Eq. 1) evidence the chemical inertness and strong stability, whereas small ionization potential denotes high activity of the atoms and molecules [59]. According to ionization potential values, order of activity can be written as: **3b**>**3a**>**3c** and **4b**>**4c**>**4d**>**4a** for gas phase. Ionization potential values of these molecules were found as 5.78, 6.18, 6.24 e for urea derivatives and 5.95, 6.08, 6.11 and 6.13 e for thiourea derivatives, respectively. **3b** and **4b** molecules are found more active than other molecules for gas and solvent phase. Because, **3b** and **4b** molecules have the lowest Ionization potential values. It can be seen from Table-2 that the highest kinetic stable for gas and water phase belongs to **3c** and **4a** molecules.

The hardness ( $\eta$ ) and softness ( $\sigma$ ) are widely used in chemistry for explaining stability of compounds. According to Maximum Hardness Principle [54], chemical hardness is a measure of the stability of chemical species. The hardness (see eq. 5) is just half the energy gap between the  $E_{\text{HOMO}}$  and  $E_{\text{LUMO}}$ . If a molecule has a large energy gap, it is called hard and other wise is called soft [61]. The active compounds have a greater softness value. Softness (see eq. 6) is a measure of the polarizability and soft molecules give more easily electrons to an electron acceptor molecule or surface [16]. On the

basis of the calculated chemical hardness and softness are given in Fig. 3. According to softness values, electron donating trend of studied chemical compounds may be written as: **3b**>**3c**>**3a** for urea derivatives **3a-c**, and **4b**>**4c**>**4d**>**4a** for thiourea derivatives **4a-d** in gas phase and **3b**>**3a**>**3c** for **3a-c**, and **4b**>**4c**>**4a**>**4d** for **4a-d** in solvent phase. **3b** and **4b** are found more active molecules for both phases.

The average values of the HOMO and LUMO energies have been defined as the chemical potential ( $\mu$ ). The chemical potential was defined as the first derivative of the total energy with respect to the number of electrons. The negative value of the chemical potential was known as the electronegativity ( $\chi$ ) (see eq. 4). Chemical potential, electronegativity and hardness are descriptors for the predictions about chemical properties of molecules [65]. The electronegativity also indicates the propensity of an inhibitor molecule to accept electrons or electron density. Electronegativity that represents the power to attract the electrons of chemical species is a useful quantity in the prediction of activity of molecules [16]. In generally, a molecule with lower electronegativity is associated with higher electron donating tendency and therefore exhibited higher activity as compare to a molecular with higher value of electronegativity [66].

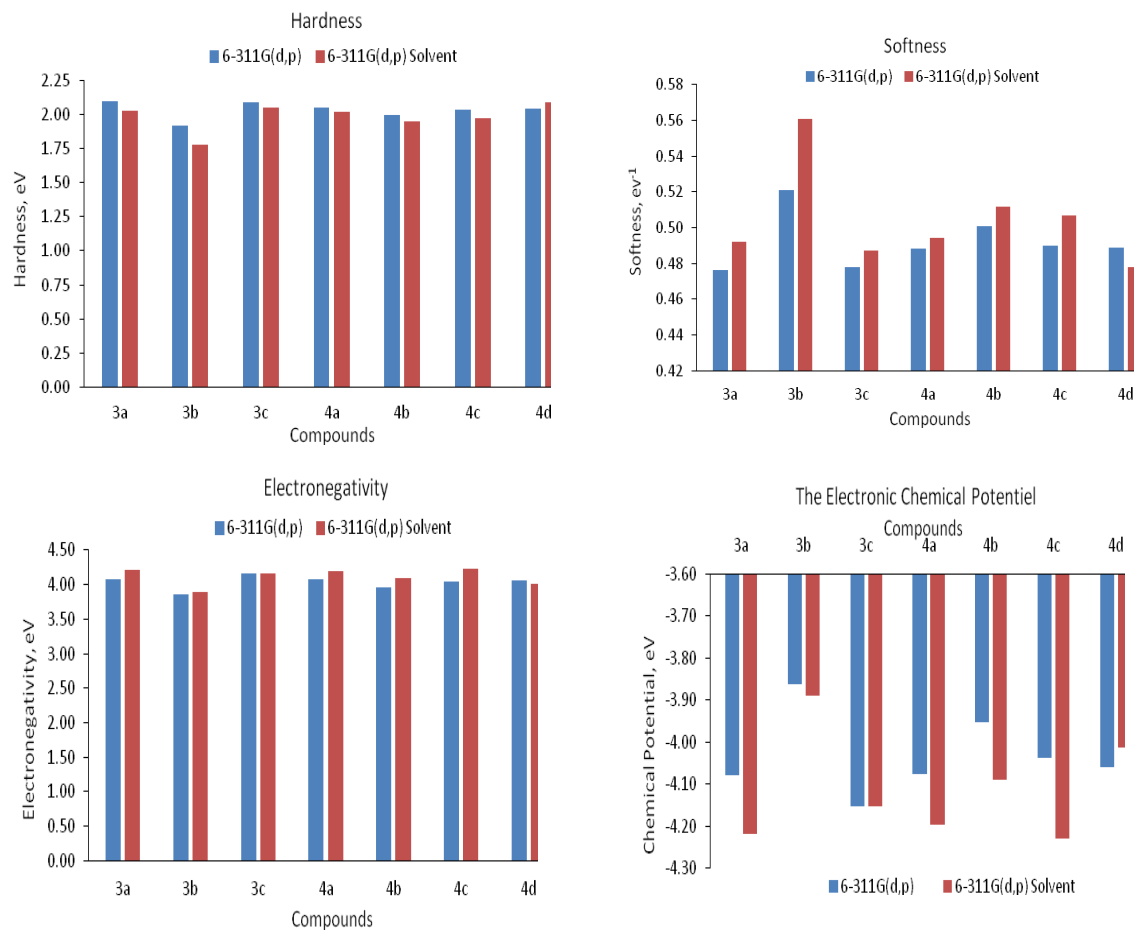


Fig. 3: The calculated some quantum chemical parameters for gas and solvent phase compounds using B3LYP/6-311G(d,p) method (solvent: acetic acid for **3c** and ethanol for other molecules).

The electronegativity values were found 4.08, 3.86, 4.15 for **3a-c** and 4.08, 3.95, 4.04, 4.06 eV for **4a-d** in gas phase, and 4.22, 3.89, 4.15 for **3a-c**, 4.20, 4.09, 4.23, 4.13 eV for **4a-d** in solvent phase, respectively. The electronegativity value of **3b** is more active than other molecules for urea derivatives **3a-c** and **4b** was found for thiourea derivatives **4a-d** in gas phase (Fig. 3).

Dipole moment (DM) is another indicator of activity of chemical compounds. Although some authors reported that there is no any remarkable relationship between dipole moment and inhibition efficiency [57, 67] and some authors showed that activity increases with the increasing of the dipole moment [68-70]. In some studies, authors supported that increasing value of dipole moment facilitates the electron transport process [69, 70]. For instance, in Table-2, calculated dipole moment values are 3.20, 4.22, 4.49 for **3a-c** molecules and 2.11, 3.13, 1.75 and 1.89 Debye for gas phase, respectively. According to dipole moment results, **3c** and **4b** were

found to be the best active for gas phase. The other results can be seen from Table-2.

Table-2: The calculated some quantum chemical parameters for gas and solvent phase of the non-protonated compounds using B3LYP/6-311G(d,p) method.

Molecule	I, eV	DM, Debye	MV, cm <sup>3</sup> /mol	TMAC, e	$\omega$ , eV
3a	6.18	3.20	331.35	-3.38	3.96
3b	5.78	4.22	311.06	-3.76	3.89
3c	6.24	4.49	306.84	-3.67	4.13
4a	6.13	2.11	413.10	-2.98	4.05
4b	5.95	3.13	369.55	-3.44	3.91
4c	6.08	1.75	435.82	-3.08	3.99
4d	6.11	1.89	407.04	-3.12	4.03
3a*	6.25	4.27	393.31	-3.37	4.38
3b*	5.67	4.60	431.29	-3.85	4.24
3c*	6.21	5.78	348.54	-3.78	4.20
4a*	6.22	4.32	322.40	-3.26	4.35
4b*	6.04	2.22	415.55	-3.68	4.28
4c*	6.20	3.41	376.26	-3.24	4.53
4d*	6.11	1.92	427.23	-3.12	4.03

\*Solvent phase: acetic acid for **3c** and ethanol for other molecules

The total of negative Mulliken atomic charges (TMAC) can be seen from Table-2. The

TMAC values have been found as -3.38, -3.76, -3.67 for **3a-c** and -2.98, -3.44, 3.08, -3.12 e for **4a-d** in gas phase, respectively. According to dipole moment results, **3b** and **4b** were found to be the best active as molecules. The negative charge densities have been shown to increase on active molecules. This result is the same as of the order of activity of gases found by other calculation methods for gas phase. The results of other calculations: global electrophilicity index ( $\omega$ ) and MV can be seen in Table-2.

DFT study can be used to better understand the molecular behaviour and structural conformation of the compounds. DFT approach helps to study the electrostatic potential (ESP) distribution of the compound more precisely [62]. Molecular Electrostatic Potential (MEP) is used to describe the electrostatic interaction between a molecule and an atom. ESP is indicating the electrophilic and nucleophilic nature of the molecules, and its essential tools to study the reactivity nature of the compounds. ESP surfaces of the compounds are shown from Fig.

4. MEP maps at the surface are represented by different colours. The blue colour in the ESP graphs, represents the maximum amount of the positive region where the nucleophilic reaction takes place and reddish region represented the negative region where the electrophilic reaction takes place [62], and green colour represents zero potential [71].

Fig. 4 shows that the electron density increases around the oxygen atoms with the negative electrostatic potential values of the molecules. Especially, most of the electrophilic reactions takes place of O11 and O18 oxygen atoms (the numbers of O11 and O18 oxygen atoms can be seen from the fig in Table-3) for notr and solvent phase of all compounds, and the red coloured region in Fig. 4 shows the maximum electronegativity. This result indicates that these atoms will enter the electrophilic reactions more easily. On the other hand, it can be seen that the electron density decreases around 24N atom with the positive electrostatic potential values of the compounds.

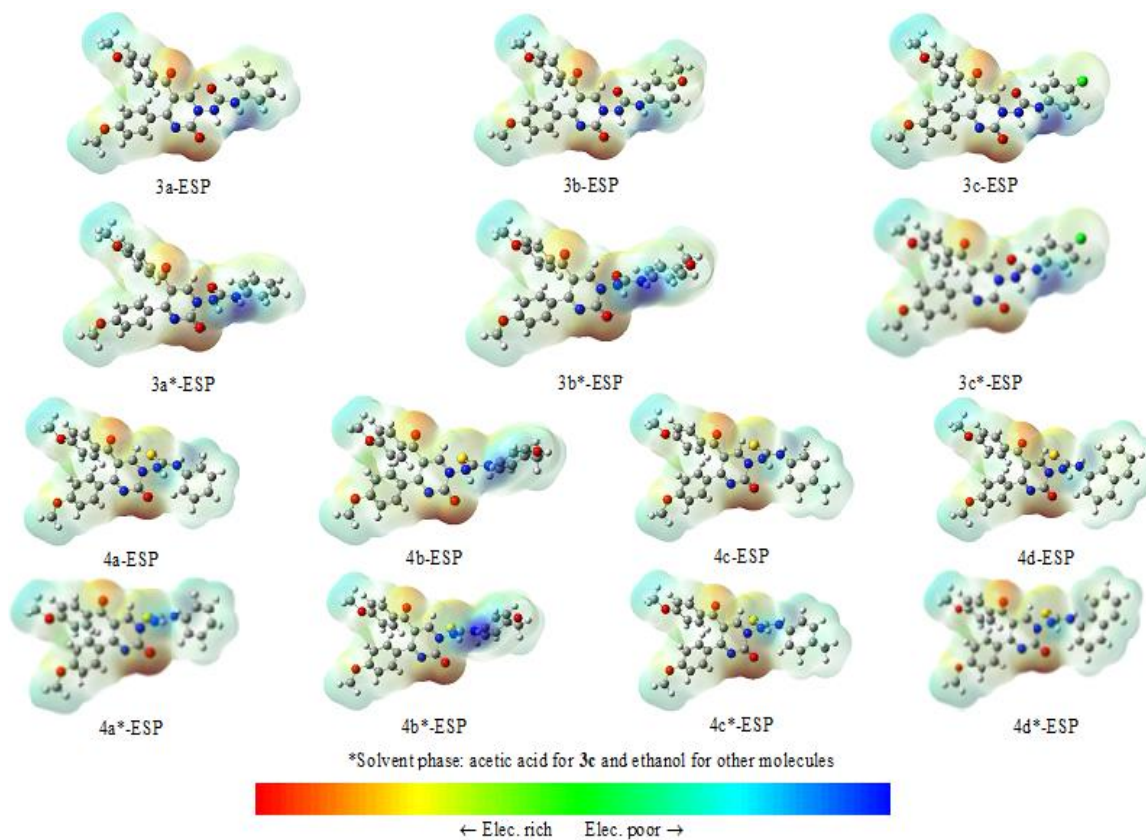
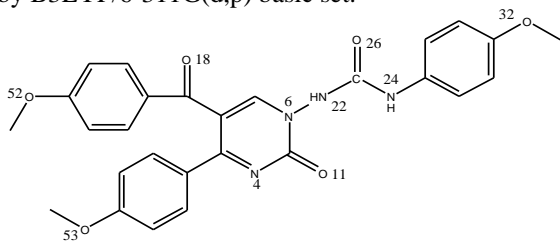


Fig. 4: Molecular electrostatic potential (MEP) surface of molecules by using DFT/B3LYP/6-311G(d,p) basic set for notr and solvent phase.

Table-3: Mulliken atomic charges (e) on nitrogen, oxygen and chlorine atoms of urea derivatives (**3a-c**) by B3LYP/6-311G(d,p) basic set.



Atom	3a	3b	3c	3a*	3b*	3c*
N4	-0.364	-0.365	-0.364	-0.396	-0.410	-0.405
N6	-0.338	-0.337	-0.339	-0.312	-0.304	-0.312
O11	-0.389	-0.388	-0.389	-0.406	-0.430	-0.419
O18	-0.319	-0.319	-0.318	-0.354	-0.388	-0.376
N22	-0.296	-0.298	-0.296	-0.323	-0.333	-0.324
N24	-0.478	-0.478	-0.480	-0.489	-0.492	-0.491
O26	-0.371	-0.376	-0.370	-0.415	-0.446	-0.421
O32	-	-0.351	-	-	-0.386	-
Cl32	-	-	-0.073	-	-	-0.103
O52	-0.340	-0.340	-0.340	-0.357	-0.367	-0.361
O53	-0.342	-0.343	-0.342	-0.361	-0.371	-0.365

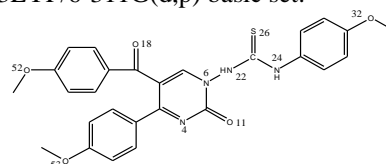
\*Solvent phase: acetic acid for **3c** and ethanol for other molecules

In such studies, electronic charge analysis for atoms in the molecules is important because binding capability of a molecule depends also on electronic charge on heteroatoms of the molecule. The binding facilitates as the negative charge on hetero atom increases [72]. In this study, we used Mulliken population analysis to calculate the atomic charges [73]. Mulliken atomic charges on nitrogen, oxygen, sulfur and chlorine atoms of molecules for non-protonated gas and solvent phase are given in Tables-3 and 4. As can be seen from Tables-3 and 4, the negative charge densities are more in the vicinity on nitrogen and oxygen atoms. The Mulliken negative charges values are generally lower in gas phase than in solvent phase for all compounds. It is easier to bind a molecule from these negative charge atoms where the negative value is higher. As a result, these atoms in molecules to be cause strong interaction.

We calculated the  $^1\text{H}$  and  $^{13}\text{C}$ -NMR chemical shifts by using Gaussian 03, Revision D.01 program [15]. The calculated  $^1\text{H}$  and  $^{13}\text{C}$ -NMR results are shown in supplementary. The experimental and calculated results are given comparatively in these tables. Since the signals of the carbon and hydrogen atoms in the pyrimidine and the phenyl ring overlap too much, they are given as the range in results of the experimental part. In addition, the hydrogen atoms of methyl, methoxy and naphthyl groups are also given as the range because of overlap. According to the data given in supp. Tables 1-7, the  $^{13}\text{C}$  chemical shifts for the pyrimidine and aromatic rings of some molecules have been recorded in the

range 171.3-113.7 ppm, and  $^1\text{H}$ -NMR chemical shifts for the aromatic ring have been recorded in the range 7.79-6.67 ppm and 8.62-8.44 ppm for the pyrimidine ring whereas the corresponding shifts have been simulated at 177.6-113.3 and 8.85-6.62 ppm at B3LYP level for the pyrimidine and aromatic rings. Also, the chemical shifts for the methoxy group carbon atoms have been observed at 56.1-55.6 ppm and simulated in the range 57.8-53.4 ppm by B3LYP level. The chemical shifts for the carbon (5C) atoms of the carbonyl group in the pyrimidine ring have been observed at 153.6-152.9 ppm and simulated in the range 161.8-155.3 ppm. It is seen that the protons of the NH- group give a signal in the range of 10.94-9.28 and simulated in the range 7.94-5.66 ppm. It is seen the other results from the supplementary tables that the experimental and calculated results are generally compatible.

Table-4: Mulliken atomic charges (e) on nitrogen, oxygen and sulfur atoms of thiourea derivatives (**4a-d**) by B3LYP/6-311G(d,p) basic set.



Atom	4a	4b	4c	4d	4a*	4b*	4c*	4d*
N4	-0.364	-0.356	-0.365	-0.364	-0.418	-0.416	-0.397	-0.364
N6	-0.330	-0.337	-0.329	-0.331	-0.309	-0.311	-0.314	-0.331
O11	-0.367	-0.384	-0.367	-0.367	-0.415	-0.425	-0.392	-0.357
O18	-0.318	-0.318	-0.318	-0.318	-0.387	-0.387	-0.362	-0.318
N22	-0.236	-0.255	-0.235	-0.233	-0.276	-0.282	-0.265	-0.233
N24	-0.411	-0.448	-0.411	-0.431	-0.414	-0.426	-0.412	-0.431
S26	-0.216	-0.173	-0.221	-0.217	-0.387	-0.366	-0.331	-0.217
O32	-	-0.347	-	-	-	-0.379	-	-
O52	-0.340	-0.340	-0.340	-0.340	-0.366	-0.366	-0.356	-0.340
O53	-0.342	-0.343	-0.342	-0.342	-0.370	-0.370	-0.360	-0.342

\*Solvent phase: acetic acid for **3c** and ethanol for other molecules

## Conclusions

A series of the new 2-oxopyrimidin-1(2H)-yl-urea (**3a-c**) and thiourea (**4a-d**) derivatives were synthesized, and their  $^1\text{H}$ -NMR,  $^{13}\text{C}$ -NMR and elemental analysis were performed. The quantum chemical parameters of synthesized compounds have been found and discussed. According to results, **3b** and **4b** molecules are found more active than other molecules for gas and solvent phase.

## Acknowledgements

Experimental part of this study was financially supported by Erciyes University Research Fund (FLY-2013-4315), and computers allocated by

the Erciyes University data center were used for quantum chemical calculations.

## References

1. D. H. Boschelli, Z. Wu, S. R. Klutchko, H. D. H. Showalter, J. M. Hamby, G. H. Lu, T. C. Major, T. K. Dahrting, B. Batley, R. L. Panek, J. Keiser, B. G. Hartl, A. J. Kraker, W. D. Klohs, B. J. Roberts, S. Patmore, W. L. Elliott, R. Steinkampf, L. A. Bradford, H. Hallak, A. M. Doherty, Synthesis and tyrosine kinase inhibitory activity of a series of 2-amino-8H-pyrido[2,3-d]pyrimidines: identification of potent, selective platelet-derived growth factor receptor tyrosine kinase inhibitors, *J. Med. Chem.*, **41**, 4365 (1998).
2. S. R. Walker, E. J. Carter, B. C. Huff, J. C. Morris, Variolins and related alkaloids, *Chem. Rev.*, **109**, 3080 (2009).
3. H. Shao, S. Shi, S. Huang, A. J. Hole, A. Y. Abbas, S. Baumli, X. Liu, F. Lam, D. W. Foley, P. M. Fischer, M. Noble, J. A. Endicott, C. Pepper, S. Wang, Substituted 4-(thiazol-5-yl)-2-(phenylamino)pyrimidines are highly active CDK9 inhibitors: synthesis, X-ray crystal structures, structure-activity relationship, and anticancer activities, *J. Med. Chem.*, **56**, 640 (2013).
4. A. R. El-Gazzar, H. N. Hafez, Synthesis of 4-substituted pyrido[2,3-d]pyrimidin-4(1H)-one as analgesic and anti-inflammatory agents, *Bioorg. Med. Chem. Lett.*, **19**, 3392 (2009).
5. B. L. Narayana, A. R. R. Rao, P. S. Rao, Synthesis of new 2-substituted pyrido[2,3-d]pyrimidin-4(1H)-ones and their antibacterial activity, *Eur. J. Med. Chem.*, **44**, 1369 (2009).
6. S. Federico, A. Ciancetta, N. Porta, S. Redenti, G. Pastorin, B. Cacciari, K. N. Klotz, S. Moro, G. Spalluto, Scaffold decoration at positions 5 and 8 of 1,2,4-Triazolo[1,5-c]Pyrimidines to explore the antagonist profiling on adenosine receptors: A preliminary structure-activity relationship study, *J. Med. Chem.*, **57**, 6201 (2014).
7. S. Sharma, Isothiocyanates in heterocyclic synthesis, *Sulfur Rep.*, **8**, 327 (1989).
8. Z. Önal, A. C. Daylan, Cyclization reaction of 1-pyrimidinyl-3-arylthiourea derivatives with oxalyl dichloride, *Asian J. Chem.*, **19**, 1455 (2007).
9. A. Saeed, R. Qamar, T. A. Fattah, U. Florke, M. F. Erben, Recent developments in chemistry, coordination, structure and biological aspects of 1-(acyl/aroyl)-3(substituted) thiourea, *Res. Chem. Intermed.*, **43**, 3053 (2017).
10. A. Saeed, U. Florke, M. F. Erben, A review on the chemistry, coordination, structure and biological properties of 1-(acyl/aroyl)-3-(substituted) thioureas, *J. Sulfur Chem.*, **35**, 318 (2013).
11. R. S. Upadhayaya, G. M. Kulkarni, N. R. Vasireddy, J. K. Vandavasi, S. Dixit, S. Sharma, V. Chattapadhyaya, Design, synthesis and biological evaluation of novel triazole, urea and thiourea derivatives of quinoline against mycobacterium tuberculosis, *Bioorg. Med. Chem.*, **17**, 4681 (2009).
12. S. A. Khan, N. Singh, K. Saleem, Synthesis, characterization and in vitro antibacterial activity of thiourea and urea derivatives of steroids, *Eur. J. Med. Chem.*, **43**, 2272 (2008).
13. P. P. Sett, R. Ranken, D. E. Robinson, S. A. Osgood, L. M. Risen, E. L. Rodgers, M. T. Migawa, E. A. Jefferson, E. E. Swayze, Aryl urea analogs with broad-spectrum antibacterial activity, *Bioorg. Med. Chem. Lett.*, **14**, 5569 (2004).
14. B. Koçyiğit-Kaymakçioğlu, S. Rollas, E. Körceğez, F. Arıcıoğlu, Synthesis and biological evaluation of new N-substituted-N'-(3,5-di/1,3,5-trimethylpyrazole-4-yl)thiourea/urea derivatives, *Eur. J. Pharm. Sci.*, **26**, 97 (2005).
15. M. J. Frisch, G. W. Trucks, H. B. Schlegel, G. E. Scuseria, M. A. Robb, J. R. Cheeseman Jr., J. A. Montgomery, T. Vreven, K. N. Kudin, J. C. Burant, J. M. Millam, S.S. Iyengar, J. Tomasi, V. Barone, B. Mennucci, M. Cossi, G. Scalmani, N. Rega, G. A. Petersson, H. Nakatsuji, M. Hada, M. Ehara, K. Toyota, R. Fukuda, J. Hasegawa, M. Ishida, T. Nakajima, Y. Honda, O. Kitao, H. Nakai, M. Klene, X. Li, J.E. Knox, H. P. Hratchian, J. B. Cross, V. Bakken, C. Adamo, J. Jaramillo, R. Gomperts, R. E. Stratmann, O. Yazyev, A. J. Austin, R. Cammi, C. Pomelli, J. W. Ochterski, P. Y. Ayala, K. Morokuma, G. A. Voth, P. Salvador, J. J. Dannenberg, V. G. Zakrzewski, S. Dapprich, A. D. Daniels, M. C. Strain, O. Farkas, D. K. Malick, A. D. Rabuck, K. Raghavachari, J. B. Foresman, J. V. Ortiz, Q. Cui, A. G. Baboul, S. Clifford, J. Cioslowski, B. B. Stefanov, G. Liu, A. Liashenko, P. Piskorz, I. Komaromi, R. L. Martin, D. J. Fox, T. Keith, M. A. Al-Laham, C. Y. Peng, A. Nanayakkara, M. Challacombe, P. M. W. Gill, B. Johnson, W. Chen, M. W. Wong, C. Gonzalez, J. Pople, Gaussian 03, Revision D.01, *Gaussian Inc.*, Wallingford, CT (2004).
16. S. Kaya, C. Kaya, L. Guo, F. Kandemirli, B. Tüzün, İ. Uğurlu, L. H. Madkour, M. Saracoglu,

- Quantum chemical and molecular dynamics simulation studies on inhibition performances of some thiazole and thiadiazole derivatives against corrosion of iron, *J. Mol. Liq.*, **219**, 497 (2016).
17. E. E. Ebenso, T. Arslan, F. Kandemirli, I. Love, C. Öğretir, M. Saracoglu and S. A. Umoren, Theoretical studies of some sulphonamides as corrosion inhibitors for mild steel in acidic medium, *Int. J. Quantum Chem.*, **110**, 2614 (2010).
  18. M. A. Amin, M. A. Ahmed, H. A. Arida, T. Arslan, M. Saracoglu and F. Kandemirli, Monitoring corrosion and corrosion control of iron in HCl by non-ionic surfactants of the TRITON-X series-Part II. Temperature effect, activation energies and thermodynamics of adsorption, *Corros. Sci.*, **53**, 540 (2011).
  19. M. A. Amin, M. A. Ahmed, H. A. Arida, F. Kandemirli, M. Saracoglu, T. Arslan and M. A. Basaran, Monitoring corrosion and corrosion control of iron in HCl by non-ionic surfactants of the TRITON-X series-Part III. Immersion time effects and theoretical studies, *Corros. Sci.*, **53**, 1895 (2011).
  20. S. Zor, M. Saracoglu, F. Kandemirli and T. Arslan, Inhibition effects of amides on the corrosion of copper in 1.0 M HCl: Theoretical and experimental studies, *Corrosion*, **67**, 12, 125003 (2011).
  21. F. Kandemirli, M. Saracoglu, G. Bulut, E. Ebenso, T. Arslan and A. Kayan, Synthesis and theoretical study of zinc(II) and nickel(II) complexes of 5-methoxyisatin 3-[N-(4-chlorophenyl)thiosemicarbazone], *ITB J. Science (J. Math. and Fund. Sci.)*, **44A**, 35 (2012).
  22. M. A. Amin, O. A. Hazzazi, F. Kandemirli and M. Saracoglu, Inhibition performance and adsorptive behaviour of three amino acids on cold rolled steel in 1.0 M HCl-chemical, electrochemical and morphological studies, *Corrosion*, **68**, 688 (2012).
  23. F. Kandemirli, M. Saracoglu, M. A. Amin, M. A. Basaran and C. D. Vurdu, The Quantum chemical calculations of serine, threonine and glutamine, *Int. J. Electrochem. Sci.*, **9**, 3819 (2014).
  24. M. A. Amin, N. El-Bagoury, M. Saracoglu and M. Ramadan, Electrochemical and corrosion behavior of cast re-containing inconel 718 alloys in sulphuric acid solutions and the effect of Cl<sup>-</sup>, *Int. J. Electrochem. Sci.*, **9**, 5352 (2014).
  25. F. Kandemirli, C. D. Vurdu, M. Saracoglu, Y. Akkaya and M. S. Cavus, Some molecular properties and reaction mechanism of synthesized isatin thiosemicarbazone and its zinc(II) and nickel(II) complexes, *Int. Res. J. Pure and Applied Chem.*, **9**, 1, (2015)
  26. N. El-Bagoury, M. A. Amin and M. Saracoglu, Effect of aging treatment on the electrochemical and corrosion behavior of nitire shape memory alloy, *Int. J. Electrochem. Sci.*, **10**, 5291, (2015).
  27. İ. Ö. İlhan, M. Çadır, M. Saracoglu, F. Kandemirli, Z. Kökbudak and S. Akkoç, The reactions and quantum chemical calculations of some pyrazole-3-carboxylic acid chlorides with various hydrazides, *Chem. Sci. Rev. Lett.*, **4**, 838 (2015).
  28. M. A. Amin, S. A. Fadlallah, G. S. Alosaimi, F. Kandemirli, M. Saracoglu, S. Szunerits and R. Boukherroub, Cathodic activation of titanium-supported gold nanoparticles: an efficient and stable electrocatalyst for the hydrogen evolution reaction, *Int. J. Hyd. Energy*, **41**, 6326 (2016).
  29. A. Tazouti, M. Galai, R. Touir, M. Ebn Touhami, A. Zarrouk, Y. Ramli, M. Saraçoğlu, S. Kaya, F. Kandemirli and C. Kaya, Experimental and theoretical studies for mild steel corrosion inhibition in 1 M HCl by three new quinoxalinone derivatives, *J. Mol. Liquids*, **221**, 815 (2016).
  30. M. A. Amin, M. Saracoglu, N. El-Bagoury, T. Sharshar, M. M. Ibrahim, J. Wysocka, S. Krakowiak and J. Ryl, Microstructure and corrosion behaviour of carbon steel and ferritic and austenitic stainless steels in NaCl solutions and the effect of p-Nitrophenyl phosphate disodium salt, *Int. J. Electrochem. Sci.*, **11**, 10029 (2016).
  31. M. Saracoglu, F. Kandemirli, A. Ozalp and Z. Kokbudak, Synthesis and quantum chemical calculations of 2,4-dioxopentanoic acid derivatives-Part I, *Chem. Sci. Rev. Lett.*, **6**, 1 (2017).
  32. M. Saracoglu, F. Kandemirli, A. Ozalp and Z. Kokbudak, Synthesis and quantum chemical calculations of 2,4-dioxopentanoic acid derivatives-part II, *Int. J. Sci. Eng. Inv.*, **6**, 50 (2017).
  33. B. Saima, A. Khan, R. Un Nisa, T. Mahmood, K. Ayub, Theoretical insights into thermal cyclophanediene to dihydropyrene electrocyclic reactions; a comparative study of Woodward Hoffmann allowed and forbidden reactions, *J. Mol. Model.*, **22**, 81 (2016).
  34. M. Saracoglu, M. I. A. Elusta, S. Kaya, C. Kaya, F. Kandemirli, Quantum chemical studies on the corrosion inhibition of Fe<sub>78</sub>B<sub>13</sub>Si<sub>9</sub> glassy alloy in Na<sub>2</sub>SO<sub>4</sub> solution of some

- thiosemicarbazone derivatives, *Int. J. Electrochem. Sci.*, **13**, 8241 (2018).
35. M. Saracoglu, Z. Kokbudak, Z. Çimen, F. Kandemirli, Synthesis and DFT Quantum Chemical Calculations of Novel Pyrazolo[1,5-c]pyrimidin-7(1H)-one Derivatives, *J. Chem. Soc. Pak.*, **41**, (It was accepted for publication) (2019).
36. M. Saracoglu, S. G. Kandemirli, A. Başaran, H. Sayiner, F. Kandemirli, Investigation of structure-activity relationship between chemical structure and CCR5 anti HIV-1 activity in a class of 1-[N-(methyl)-N-(phenylsulfonyl)amino]-2-(phenyl)-4-[4-(substituted)piperidin-1-yl] butanes derivatives: The electronic-topological approach, *Curr. HIV Res.*, **9**, 300 (2011).
37. M. Saracoglu, F. Kandemirli, M. A. Amin, C. D. Vurdu, M. S. Cavus, G. Sayiner, The quantum chemical calculations of some thiazole derivatives, Proceedings of the 3<sup>rd</sup> International Conference on Computation for Science and Technology (ICCST-3), *Published by Atlantis Press*, **5**, 149 (2015).
38. K. F. Khaled, Studies of iron corrosion inhibition using chemical, electrochemical and computer simulation techniques, *Electrochim. Acta*, **55**, 6523 (2010).
39. M. J. Dewar, W. Thiel, Ground states of molecules. 38. The MNDO method. Approximations and parameters, *J. Am. Chem. Soc.*, **99**, (1977) 4899.
40. R. G. Pearson, Hard and soft acids and bases- the evolution of a chemical concept, *Coord. Chem. Rev.*, **100**, 403 (1990).
41. L. Pauling, The Nature of the Chemical Bond, *Cornell University Press*, Ithaca, New York, (1960).
42. R. G. Parr, R. G. Pearson, Absolute hardness: companion parameter to absolute electronegativity, *J. Am. Chem. Soc.*, **105**, 7512 (1983).
43. P. K. Chattaraj, U. Sarkar, D. R. Roy, Electrophilicity index, *Chem. Rev.*, **106**, 2065 (2006).
44. E. E. Ebenso, M. M. Kabanda, T. Arslan, M. Saracoglu, F. Kandemirli, L. C. Murulana, A. K. Singh, S. K. Shukla, B. Hammouti, K. F. Khaled, M. A. Quraishi, I. B. Obot, N. O. Edd, Quantum chemical investigations on quinoline derivatives as effective corrosion inhibitors for mild steel in acidic medium, *Int. J. Electrochem. Sci.*, **7**, 5643 (2012).
45. E. Saripinar, Y. Güzel, Z. Önal, İ. Ö. İlhan, Y. Akcamur, 4-(-4-methoxybenzoyl)-5-(-4-methoxyphenyl)-2,3-dihydro-2,3-furandione, its synthesis, thermolysis and diels-alder reactions with schiff bases: experimental data and calculations, *J. Chem. Soc. Pak.*, **22**, 308 (2000).
46. L. Santos, L. A. Lima, V. Cechinel-Filho, R. Correa, F. C. Buzzi, R. J. Nunes, Synthesis of new 1-phenyl-3-(4-[(2E)]-3-phenylprop-2-enoyl]phenyl)-thiourea and urea derivatives with anti-nociceptive activity, *Bioorg. Med. Chem.*, **16**, 8526 (2008).
47. H. S. Zhang, K. Y. Zhang, L. C. Chen, Y. X. Li, L. Q. Chai, Crystal structure, spectral property, antimicrobial activity and DFT calculation of N-(coumarin-3-yl)-N'-(2-amino-5-phenyl-1,3,4-thiadiazol-2-yl) urea, *J. Mol. Struct.*, **1145**, 32 (2017).
48. H. Özay, M. Yıldırım, Ö. Özay, Synthesis and characterization of novel urea and thiourea substitute cyclotriphosphazene compounds as naked-eye sensors for F<sup>-</sup> and CN<sup>-</sup> anions, *Turk. J. Chem.*, **39**, 777 (2015).
49. A. Y. Musa, A. H. Kadhun, A. B. Mohamad, A. B. Rohoma, H. Mesmari, Electrochemical and quantum chemical calculations on 4,4-dimethyloxazolidine-2-thione as inhibitor for mild steel corrosion in hydrochloric acid, *J. Mol. Struct.*, **969**, 233 (2010).
50. K. F. Khaleda, M. M. Al-Qahtani, The inhibitive effect of some tetrazole derivatives towards Al corrosion in acid solution: Chemical, electrochemical and theoretical studies, *Mater. Chem. Phys.*, **113**, 150 (2009).
51. Y. C. Guan Luo, K. N. Han, Corrosion Inhibition of a Mild Steel by Aniline and Alkylamines in Acidic Solutions, *Corrosion*, **54**, 721 (1998).
52. S. Martinez, I. Štagljar, Correlation between the molecular structure and the corrosion inhibition efficiency of chestnut tannin in acidic solutions, *J. Mol. Struct.*, **640**, 167 (2003).
53. N. O. Obi-Egbedi, I. B. Obot, M. I. El-Khaiary, Quantum chemical investigation and statistical analysis of the relationship between corrosion inhibition efficiency and molecular structure of xanthene and its derivatives on mild steel in sulphuric acid, *J. Mol. Struct.*, **1002**, 86 (2011).
54. I. B. Obot, N. O. Obi-Egbedi, Adsorption properties and inhibition of mild steel corrosion in sulphuric acid solution by ketoconazole: Experimental and theoretical investigation, *Corros. Sci.*, **52**, 198 (2010).
55. M. M. Solomon, S. A. Umoren, I. I. Udosoro, A. P. Udoh, Inhibitive and adsorption behaviour of carboxymethyl cellulose on mild steel corrosion in sulphuric acid solution, *Corros. Sci.*, **52**, 1317 (2010).

56. A. Rauk, *Orbital interaction theory of organic chemistry*, 2nd ed; Wiley & Sons: New York (2001).
57. M. Djenane, S. Chafaa, N. Chafai, R. Kerkour, A. Hellal, Synthesis, spectral properties and corrosion inhibition efficiency of new ethyl hydrogen [(methoxyphenyl) (methylamino) methyl] phosphonate derivatives: Experimental and theoretical investigation, *J. Mol. Struct.*, **1175**, 398 (2019).
58. J. Bhawsar, P. Jain, M. G. Valladares-Cisneros, C. Cuevas-Arteaga, M. R. Bhawsar, Quantum chemical assessment of two natural compounds: Vasicine and Vasicinone as green corrosion inhibitors, *Int. J. Electrochem. Sci.*, **13**, 3200 (2018).
59. I. B. Obot, N. O. Obi-Egbedi, A. O. Eseola, Anticorrosion potential of 2-Mesityl-1H-imidazo[4,5-f][1,10]phenanthroline on mild steel in sulfuric acid solution: experimental and theoretical study, *Ind. Eng. Chem. Res.*, **50**, 2098 (2011).
60. I. B. Obot, N. O. Obi-Egbedi, E. E. Ebenso, A. S. Afolabi, E. E. Oguzie, Experimental, quantum chemical calculations, and molecular dynamic simulations insight into the corrosion inhibition properties of 2-(6-methylpyridin-2-yl)oxazolo[5,4-f][1,10]phenanthroline on mild steel, *Res. Chem. Intermed.*, **39**, 1927 (2013).
61. R. G. Parr, P. K. Chattaraj, Principle of maximum hardness, *J. Am. Chem. Soc.*, **113**, 1854 (1991).
62. D. Bhattacharjee, T. K. Devi, R., Dabrowski, A. Bhattacharjee, Birefringence, polarizability order parameters and DFT calculations in the nematic phase of two bent-core liquid crystals and their correlation, *J. Mol. Liq.*, **271**, 239 (2018).
63. R. G. Pearson, The principle of maximum hardness, *Acc. Chem. Res.*, **26**, 250 (1993).
64. R. G. Pearson, Absolute electronegativity and hardness correlated with molecular orbital theory, *Proceedings of the National Academy of Sciences of the United States of America*, **83**, 8440 (1986).
65. A. Özalp, Z. Kökbudak, M. Saracoglu, F. Kandemirli, İ. Ö. İlhan, C. D. Vurdu, The reactions and quantum chemical calculations of some pyrazole-3-carboxylic acid chlorides with various hydrazides, *Chem. Sci. Rev. Lett.*, **4**, 719 (2015).
66. C. Verma, M. A. Quraishi, K. Kluza, M., Makowska-Janusik, L. O. Olasunkanmi, E. E. Ebenso, Corrosion inhibition of mild steel in 1M HCl by D-glucose derivatives of dihydropyrido [2,3-d:6,5-d'] dipyrimidine-2, 4, 6, 8(<sup>1</sup>H, <sup>3</sup>H, <sup>5</sup>H, <sup>7</sup>H)-tetraone, *Sci. Rep.*, **7**, 44432-1 (2017).
67. R. G. Parr, L. V. Szentpaly, S. Liu, Electrophilicity index, *J. Am. Chem. Soc.*, **121**, 1922 (1999).
68. G. Gao, C. Liang, Electrochemical and DFT studies of  $\beta$ -amino-alcohols as corrosion inhibitors for brass, *Electrochim. Acta*, **52**, 4554 (2007).
69. M. Sahin, G. Gece, F. Karci, S. Bilgic, Experimental and theoretical study of the effect of some heterocyclic compounds on the corrosion of low carbon steel in 3.5% NaCl medium, *J. Appl. Electrochem.*, **38**, 809 (2008).
70. M. A. Quraishi, R. Sardar, Hector bases – a new class of heterocyclic corrosion inhibitors for mild steel in acid solutions, *J. Appl. Electrochem.*, **33**, 1163 (2003).
71. N. Khatire-Hamdi, M. Makhloufi-Chebli, H. Grib, M. Brahimi, A. M. S. Silva, Synthesis DFT/TD-DFT theoretical studies and experimental solvatochromic shift methods on determination of ground and excited state dipole moments of 3-(2-hydroxybenzoyl) coumarins, *J. Mol. Struct.*, **1175**, 811 (2019)
72. G. Gece, The use of quantum chemical methods in corrosion inhibitor studies, *Corros. Sci.*, **50**, 2981 (2008).
73. J. N. Murrell, S. F. Kettle, J. M. Tedder, The Chemical Bond, *John Wiley & Sons*, Chichester, UK (1985).